

UCSF

UC San Francisco Previously Published Works

Title

Moderate Ischemic Mitral Regurgitation After Posterolateral Myocardial Infarction in Sheep Alters Left Ventricular Shear but Not Normal Strain in the Infarct and Infarct Borderzone

Permalink

<https://escholarship.org/uc/item/3s81m7qk>

Journal

The Annals of Thoracic Surgery, 101(5)

ISSN

0003-4975

Authors

Ge, Liang

Wu, Yife

Soleimani, Mehrdad

et al.

Publication Date

2016-05-01

DOI

10.1016/j.athoracsur.2015.10.083

Peer reviewed



Published in final edited form as:

Ann Thorac Surg. 2016 May ; 101(5): 1691–1699. doi:10.1016/j.athoracsur.2015.10.083.

Moderate ischemic mitral regurgitation after postero-lateral myocardial infarction in sheep alters left ventricular shear but not normal strain in the infarct and infarct borderzone

Liang Ge, PhD^{1,3,6}, Yife Wu, BS⁶, Mehrdad Soleimani, MD⁶, Michael Khazalpour, MD⁶, Kiyooki Takaba, MD⁶, Mehrzad Tartibi, PhD⁶, Zhihong Zhang, MS⁶, Gabriel Acevedo-Bolton, PhD^{5,6}, David A. Saloner, PhD^{5,6}, Arthur W. Wallace, MD, PhD^{2,6}, Rakesh Mishra, MD^{4,6}, Eugene A. Grossi, MD⁷, Julius M. Guccione, PhD^{1,3,6}, and Mark B. Ratcliffe, MD^{1,3,6}

¹Department of Surgery, University of California, San Francisco, California

²Department of Anesthesia, University of California, San Francisco, California

³Department of Bioengineering, University of California, San Francisco, California

⁴Department of Medicine, University of California, San Francisco, California

⁵Department of Radiology, University of California, San Francisco, California

⁶Veterans Affairs Medical Center, San Francisco, California

⁷Department of Cardiothoracic Surgery, NYU School of Medicine, New York, New York

Abstract

Background—Chronic ischemic mitral regurgitation (CIMR: MR) is associated with poor outcome. Left ventricular (LV) strain after postero-lateral myocardial infarction (MI) may drive LV remodeling. Although moderate CIMR has been previously shown to effect LV remodeling, the effect of CIMR on LV strain after postero-lateral MI remains unknown. We tested the hypothesis that moderate CIMR alters LV strain after postero-lateral MI.

Methods/Results—Postero-lateral MI was created in 10 sheep. Cardiac MRI with tags was performed 2 weeks before and 2, 8 and 16 weeks after MI. LV and right ventricular (RV) volumes were measured and regurgitant volume indexed to body surface area (BSA; *Regurg Volume Index*) calculated as the difference between LV and RV stroke volumes / BSA. Three-dimensional strain was calculated.

Circumferential (E_{cc}) and longitudinal (E_{ll}) strains were reduced in the infarct proper, MI borderzone (BZ) and remote myocardium 16 weeks after MI. In addition, radial circumferential (E_{rc}) and radial longitudinal (E_{rl}) shear strains were reduced in remote myocardium but increased in the infarct and BZ 16 weeks after MI. Of all strain components, however, only E_{rc} was effected by *Regurg Volume Index* ($p=0.0005$). There was no statistically significant effect of *Regurg Volume Index* on E_{cc} , E_{ll} , E_{rl} , or circumferential longitudinal shear strain (E_{cl}).

Conclusions—Moderate CIMR alters radial circumferential shear strain after postero-lateral MI in the sheep. Further studies are needed to determine the effect of shear strain on myocyte hypertrophy and the effect of mitral repair on myocardial strain.

Introduction

Mitral regurgitation (MR) associated with postero-lateral myocardial infarction (MI; CIMR) affects 1.2 to 2.1 million patients in the United States with more than 400,000 patients having moderate-to-severe MR. [1] In patients with mild left ventricular (LV) enlargement, moderate CIMR increases the incidence of heart failure from 18 to 68% [2] and mortality from 39 to 62%. [3]

CIMR is caused by leaflet restriction and annular enlargement. Leaflet restriction is due to remodeling of the postero-lateral LV wall which makes the posterior papillary muscle move relative to the mitral valve and thereby restricts mitral leaflet motion. [4]

There is significant controversy about the added effect of CIMR on post-MI LV remodeling and the ability of mitral repair (MVR) to reverse LV remodeling after postero-lateral MI. There are animal studies for [5-7] and against [8] an effect on post-MI remodeling and for [9] and against [10] an effect of MVR. Further, in patients, while the NIH supported CTS Net study of MVR for moderate CIMR found no benefit [11], application of the Coapsys device in patients with moderate CIMR was associated with a survival advantage. [12]

Knowledge of regional myocardial strain (deformation of a body with regard to its reference configuration), stress and contractility will help us understand LV remodeling and the development of CIMR. First, it is likely that high strain and associated high stress in the myocardium may act as a trigger for post-MI LV remodeling [13]. Second, high fidelity strain measurement are necessary to construct computation models of the LV after postero-lateral MI that are able to calculate the effect of CIMR on regional contractility. [14]

The effect of CIMR on 3D regional LV strain has not been previously measured. We used MRI with non-invasive cardiac tags [15] to calculate three-dimensional strain and to more accurately measure LV and regurgitant volumes. We tested the hypotheses moderate CIMR alters LV strain after postero-lateral MI in sheep.

Methods

Animals used in this study were treated under a protocol approved by the San Francisco VA Medical Center's Institutional Animal Care and Use Committee and in compliance with the "Guide for the Care and Use of Laboratory Animals" prepared by the Institute of Laboratory Animal Resources, National Research Council, and published by the National Academy Press, revised 1996.

Myocardial Infarction

Adult sheep underwent left thoracotomy and postero-lateral MI as previously described. [16] Briefly, when there were 4 obtuse marginal (OM) coronary branches, OM2 and OM3 were

ligated. [16] However, it was fairly common for a sheep to have a large branched OM1 and, in that case, the posterior branch of OM1 and OM2 were ligated.

Magnetic resonance imaging

Two weeks before MI and 2, 8 and 16 weeks after MI, echocardiography and cardiac MRI were performed as previously described. [17] Cardiac MRI was performed using non-invasive tags as previously described. [15] Isoflurane level and end tidal CO₂ were monitored during the MRI. Isoflurane was maintained at 2% by infrared spectrophotometry and end tidal CO₂ was kept between 25 and 30. In addition, if necessary, an infusion of neosynephrine was titrated to keep systemic blood pressure at 90 mm Hg.

Image Analysis

Contouring and surfacing of the LV and RV were performed as previously described. [18] The borderzone (BZ)/ MI interface was identified on cine MRI images. The BZ was defined as extending 1 cm from the infarct edge. 3D volumes of the LV and RV were calculated by piecewise integration of the space enclosed by the epicardial and endocardial surfaces throughout the cardiac cycle. End diastole (ED) and end systole (ES) were calculated as previously described. [6]

The regurgitant volume (RegurgVolume) was calculated as the difference between the LV and RV stroke volume and regurgitant fraction (RegurgFraction) was calculated. [6] LV volume at ED and ES and RegurgVolume were indexed to body surface area (BSA). [19]

The American Society of Echocardiography (ASE) recommendations for MR severity were followed [20] with values indexed to take animal BSA into consideration. Specifically, low moderate MR in a human is defined by the ASE as a regurgitant fraction between 30 and 39% and a regurgitant volume between 30 and 44 ml. [20] Assuming that the average adult human BSA equals 1.79 m² [21], RegurgVolume Index for low moderate MR in sheep would range from 16.8 to 24.5 ml/ m².

Strain calculation

MRI tag post processing was performed as previously described. [22] Next, strain was calculated using a four-dimensional B-spline based motion tracking technique. [23] All six nonlinear, Lagrangian (Green's) strain tensor components referred to cardiac coordinates (i.e., circumferential, longitudinal, and radial) at 36 locations (12 sectors and 3 layers) in each short-axis plane/slice after correcting for through-plane motion were calculated (**Figure 1**). However, only strain from the middle layer is presented in the manuscript.

Post-mortem examination

Sheep were sacrificed one week after the 16 week MRI. LV and MI areas (**Figure 2**) were determined and the percent MI area calculated. [10]

Statistical Analysis

All values are expressed as mean ± standard deviation. The significance level was set at P<0.05.

A multivariate mixed effect analysis (Proc Mixed, SAS version 9.2, SAS Institute Inc., Cary, NC) was performed. The following regression model was used::

$$Strain = Time + Region + RegurgVolume_i \quad (1)$$

where the dependent variable, *Strain*, is E_{cc} , E_{ll} or one of the 3 regional LV shear strains, *Time* is time after MI, *Region* is a dummy variable coded for remote, borderzone and infarct regions, and *RegurgVolume_i* is RegurgVolume indexed to BSA. [19] Individual sheep were included as a random effect. All cross terms were initially included and terms that were not significant were sequentially eliminated in a backwards fashion. [24]

RegurgVolume was also treated as a dichotomous variable. In that case, a dummy variable, Mild/Mod, was equal to 1 if RegurgVolume Index averaged over the 3 post-MI data points was $> 10 \text{ ml/m}^2$.

Results

Ten sheep underwent standard postero-lateral MI. One sheep died during MI from ventricular arrhythmias. Nine sheep completed the protocol.

Sheep weight, LV pressure and LV volume are seen in **Table 1**. Please note that the data in **Table 1** has been previously presented. [6]

Sheep weight remained relatively constant until week 8 but then increased to 67.0 kg at 16 weeks (12.8%; $p < 0.0001$). The average BSA calculated for all sheep and all time points using Equation 5 was 1.26 m^2 . The relationship between end-diastolic LV volume and both weight and BSA were equally significant ($p = 0.00157$ and $p = 0.00133$ respectively). Therefore and as above, LV volume and regurgitant volumes were indexed to BSA for statistical analysis.

LV pressure at ED and ES after postero-lateral MI is seen in Table 1. LV pressure at ES was maintained near 90 mm Hg during data collection ($p = \text{NS}$). The LV pressure at ED increased from 5.1 ± 1.5 to 6.9 ± 1.5 mm Hg at 2 weeks but then remained constant ($p = \text{NS}$).

Percent infarct area was $22\% \pm 7\%$.

MR

Animals were divided into Moderate (average RegurgVolume index > 10 ; $n = 5$) and Mild RegurgVolume index (average RegurgVolume Index < 10 ; $n = 4$) groups. **Figure 3** shows the development of RegurgVolume index over time in the Mild and Moderate MR groups. There was cross over by one animal in each group. However, in general, there was separation between groups. Please note that the data in **Figure 3** has been previously presented. [6]

Changes in regional strain

Figure 4 A and B and **Table 2** shows the progression of strain in the circumflex and longitudinal directions over 16 weeks after postero-lateral MI. Two weeks after MI, E_{cc} was decreased in the infarct (-72.1% , $p < 0.0001$), BZ (-66.1% , $p < 0.0001$) and remote regions

(-46.4%, $p < 0.0001$). E_{cc} in the infarct zone remained depressed. E_{cc} in the BZ (-49.1%, $p < 0.0001$) remote zone (-25.6%, $p < 0.0001$) improved but did not regain normal values. All percents and statistics are with respect to pre infarct control.

E_{ll} was decreased in infarct (-82.4%, $p < 0.0001$), BZ (-59.8%, $p < 0.0001$) and remote regions (-56.2%, $p < 0.0001$) 2 weeks after MI. E_{ll} in all zones improved 8 weeks but E_{ll} in the infarct (-63.2%, $p = 0.0005$), BZ (-30.5%, $p = 0.0211$) and remote zones ((-42.7%, $p < 0.0001$) were once again decreased at 16 weeks.

Changes in regional shear strain

Figure 4 C and D and **Table 3** show the progression of E_{rc} , E_{rl} , and E_{cl} shear strains after postero-lateral MI. E_{rc} in the infarct, BZ and remote zones was decreased at 2 weeks, increased then increased at 8 weeks. At 16 weeks, E_{rc} in the infarct (-47.4%, $p = \text{NS}$) and remote zones (-62.5%, $p < 0.0001$) remained moderately decreased while E_{rc} in the BZ (-7.1%, $p = \text{NS}$) had returned almost to pre-infarct levels.

Change in E_{rl} and E_{cl} was less clear. E_{rl} had a 100% increase ($p = 0.0485$) was increased in the remote zone 16 weeks after MI. However, the absolute values were very small. E_{rl} in the infarct and BZ zones were not significantly changed. E_{cl} in the infarct, BZ and remote myocardium were not significantly different 16 weeks after MI. Once again, changes in percent and significance are with respect to pre infarct control.

Effect of MR

Figures 5 and 6 show circumferential and longitudinal and radial circumferential shear strain after posterolateral MI with separate plots for groups of animals with Moderate (average $\text{RegurgVolume}_i \geq 10$; $n = 5$) and Mild RegurgVolume index (average $\text{RegurgVolume}_i < 10$; $n = 4$). Note, however, that RegurgVolume Index was used as a continuous variable to calculate the statistical effect of CIMR.

Of all strain components, only E_{rc} was effected by RegurgVolume index ($p = 0.0005$; **Figure 5**) where E_{rc} shear strain in increased in the BZ at 8 and 16 weeks and in the infarct at 8 weeks. There was no statistically significant effect of RegurgVolume index on the other shear strains E_{rl} , or circumferential longitudinal shear strain (E_{cl}).

There was no statistically significant effect of RegurgVolume index on E_{cc} , E_{ll} (**Figure 6**). There was a reduction in circumferential strain in the infarct at 8 weeks and a reduction in longitudinal strain in the infarct at 16 weeks but these changes were not significant.

Discussion

The principal finding of the study is that, although circumferential and longitudinal strains and radial circumferential (E_{rc}) and radial longitudinal shear strains are altered after postero-lateral MI in sheep, only E_{rc} is effected by CIMR.

Strain in the BZ after MI

Our findings are in general agreement with prior studies of myocardial strain after postero-lateral MI. [25] For instance, Kramer and colleagues showed that 2 dimensional systolic strain in the circumferential and longitudinal directions was reduced in the BZ after antero-apical MI. [25] Similar to our findings, strain was maximally reduced early after MI but there was partial recovery of strain in the BZ noted at 8 weeks and 6 months. [25]

Pilla and colleagues measured 3D principal strain in the infarct, BZ and remote myocardium of the LV after lateral wall MI in a pig model [26] and found reductions in magnitude of the maximum principal strain (wall thickening) in all regions and changes in direction of maximum principal strain in the BZ and MI that were progressive over 4 weeks after MI. They also found changes in the magnitude and direction of the minimum principal strain (myofiber shortening) in all regions. Similar to our study, myofiber shortening improved significantly in all regions 4 weeks after MI. [26]

The effect of moderate CIMR

It is reasonable to think that the added LV volume associated with CIMR would increase myocardial strain and stress at ED with a resultant increase in eccentric LV hypertrophy. However, there is animal and human data both for [5-7, 12] and against [8, 11] and effect of CIMR on remodeling and at the current time the effect of CIMR on remodeling is an open question.

Rodriguez and colleagues found that E_{rc} was increased acutely after circumflex coronary artery occlusion in the sheep. [13, 27] Those authors suggested that increased radial circumferential shear and fiber sheet strain would act as a trigger for borderzone remodeling. [13] However, to our knowledge, there have been no studies that relate shear strain or stress per se to myocyte or LV hypertrophy. On the other hand, it is interesting that the shear strain that Rodriguez et al identified [13] is the same component that we found to be further increased with CIMR.

It is likely that E_{rc} is also related to LV torsion and recoil. When a rod undergoes torsion, the only resultant stress is shear stress in the rod cross-section that is perpendicular to the long axis. [28] To our knowledge, there are no experimental studies that relate E_{rc} to LV torsion. However, Tibiyan et al. measured LV torsion in sheep with CIMR after postero-lateral MI. Sheep with CIMR had increased maximum systolic torsion in all regions although the differences were not significant. [7]

Last is the question of whether MVR is able to reverse LV remodeling and whether the effect is mediated by a change in E_{rc} . Zuern et al used echo based speckle tracking measurement of LV strain and found that an increase in global longitudinal strain was significantly correlated with successful percutaneous repair. [29] To our knowledge, there have been no reports of shear strain after mitral repair.

Contractility in the BZ

As discussed above, high fidelity strain measurement is necessary for computational modeling studies of LV remodeling and the effect of CIMR. In a previous landmark paper,

Jackson and colleagues previously described BZ strain and remodeling in the normally perfused BZ after antero-apical MI in sheep. [30] Subsequently, Guccione and colleagues used a finite element (FE) model of the LV to show that the mechanical dysfunction in the BZ was not due to an increase in wall stress but rather to an intrinsic reduction in BZ contractility. [31] More recently, Shimkunas et al from our group used finite element methods to show that BZ contractility is also depressed after postero-lateral MI in sheep. [14] Because of their complexity, 3D strain measurements are inherently difficult to understand. However, it is important to note that the studies by Guccione [31] and Shimkunas [14] determined BZ contractility by adjusting FE model parameters until FE model output matched MRI measured strain and those studies would not have been possible without strain measurement of the type in the current study.

The cause of reduced BZ contractility is unclear but is likely mediated by high stress and strain in the borderzone myocardium. High systolic stress and positive strain in the BZ initiates myocyte apoptosis [32, 33] and activation of MMPs 2 and 9. [34, 35] Activated MMP2 has been shown to directly damage the intracellular contractile proteins myocin light chain 1 and troponin I. [36, 37]

Limitations

The thickness of the MI region after postero-lateral MI in sheep is approximately 5 mm. [38] Non invasive tags in our study were 5 mm apart so at least one tag tangential to the wall is present in the short axis plane of the MI zone. However, the number of tags in the corresponding orthogonal directions would be much greater.

It is important to realize that the B spline based method ('tt') developed by Ozturk uses the entire tag line. [23] This can clearly be seen in Figures 6 (tag displacement) and 13 (strain field) of Ozturk et al. [23] This allows for much higher spatial resolution than if only tag intersections were followed.

It is possible that other methods of strain measurement including DENSE may improve the spatial resolution of strain measurement. [39] This may be particularly important when measuring strain in the infarct borderzone. We are currently in the process of comparing results from conventional tagged MRI and DENSE in the same ovine model.

Conclusion

Circumferential and longitudinal strains and radial circumferential (Erc) and radial longitudinal shear strains are altered after postero-lateral MI in sheep, only Erc is effected by CIMR.

Further studies are needed to determine the effect of shear strain on myocyte hypertrophy. For instance, biaxial stretching of cells in culture has been performed [40] and an apparatus to provide mechanical shear strain could likely be designed. Further studies are also needed to determine the effect of mitral valve repair on ventricular shear strain.

Acknowledgments

This study was supported by NIH grants R01-HL-084431 (Dr. Ratcliffe) and R01-HL-077921 (Dr. Guccione).

Table of Abbreviations (Listed in order of appearance in the manuscript)

CIMR	Chronic ischemic mitral regurgitation
MR	Mitral regurgitation
LV	Left ventricle
MI	Myocardial infarction
MRI	Magnetic resonance imaging
RV	Right ventricle
BSA	Body surface area
RegurgVolume index	Regurgitant volume indexed to BSA
E_{cc}	Strain in the circumferential direction
E_{ll}	Strain in the circumferential direction
E_{rc}	Shear strain in the radial circumferential plane
E_{rl}	Shear strain in the radial circumferential plane
E_{cl}	Shear strain in the circumferential radial plane
BZ	Borderzone
MVR	Mitral valve repair or replacement
OM	Obtuse marginal coronary artery
ED	End-diastole
ES	End-systole

References

1. Gorman, RC.; Gorman, JH., 3rd; Edmunds, LH, Jr. Ischemic mitral regurgitation in cardiac surgery in the adult. In: Cohn, LH.; Edmunds, LH., Jr., editors. Cardiac Surgery in the adult. McGraw-Hill; New York: 2003. p. 1751-70.
2. Grigioni F, Detaint D, Avierinos JF, Scott C, Tajik J, Enriquez-Sarano M. Contribution of ischemic mitral regurgitation to congestive heart failure after myocardial infarction. *J Am Coll Cardiol.* 2005; 45(2):260–7. [PubMed: 15653025]
3. Grigioni F, Enriquez-Sarano M, Zehr KJ, Bailey KR, Tajik AJ. Ischemic mitral regurgitation: long-term outcome and prognostic implications with quantitative Doppler assessment. *Circulation.* 2001; 103(13):1759–64. [PubMed: 11282907]
4. Liel-Cohen N, Guerrero JL, Otsuji Y, Handschumacher MD, Rudski LG, Hunziker PR, et al. Design of a new surgical approach for ventricular remodeling to relieve ischemic mitral regurgitation: insights from 3-dimensional echocardiography. *Circulation.* 2000; 101(23):2756–63. [PubMed: 10851215]
5. Beeri R, Yosefy C, Guerrero JL, Nesta F, Abedat S, Chaput M, et al. Mitral regurgitation augments post-myocardial infarction remodeling failure of hypertrophic compensation. *J Am Coll Cardiol.* 2008; 51(4):476–86. [PubMed: 18222360]

6. Soleimani M, Khazalpour M, Cheng G, Zhang Z, Acevedo-Bolton G, Saloner DA, et al. Moderate mitral regurgitation accelerates left ventricular remodeling after posterolateral myocardial infarction. *Ann Thorac Surg.* 2011; 92(5):1614–20. [PubMed: 21945222]
7. Tibayan FA, Rodriguez F, Langer F, Zasio MK, Bailey L, Liang D, et al. Alterations in left ventricular torsion and diastolic recoil after myocardial infarction with and without chronic ischemic mitral regurgitation. *Circulation.* 2004; 110(11 Suppl 1):II109–14. [PubMed: 15364848]
8. Guy TS 4th, Moainie SL, Gorman JH 3rd, Jackson BM, Plappert T, Enomoto Y, et al. Prevention of ischemic mitral regurgitation does not influence the outcome of remodeling after posterolateral myocardial infarction. *J Am Coll Cardiol.* 2004; 43(3):377–83. [PubMed: 15013117]
9. Beeri R, Yosefy C, Guerrero JL, Abedat S, Handschumacher MD, Stroud RE, et al. Early repair of moderate ischemic mitral regurgitation reverses left ventricular remodeling: a functional and molecular study. *Circulation.* 2007; 116(11 Suppl):I288–93. [PubMed: 17846319]
10. Matsuzaki K, Morita M, Hamamoto H, Noma M, Robb JD, Gillespie MJ, et al. Elimination of ischemic mitral regurgitation does not alter long-term left ventricular remodeling in the ovine model. *Ann Thorac Surg.* 2010; 90(3):788–94. [PubMed: 20732497]
11. Smith PK, Puskas JD, Ascheim DD, Voisine P, Gelijns AC, Moskowitz AJ, et al. Surgical treatment of moderate ischemic mitral regurgitation. *N Engl J Med.* 2014; 371(23):2178–88. [PubMed: 25405390]
12. Grossi EA, Patel N, Woo YJ, Goldberg JD, Schwartz CF, Subramanian V, et al. Outcomes of the RESTOR-MV Trial (Randomized Evaluation of a Surgical Treatment for Off-Pump Repair of the Mitral Valve). *J Am Coll Cardiol.* 2010; 56(24):1984–93. [PubMed: 21126639]
13. Rodriguez F, Langer F, Harrington KB, Cheng A, Daughters GT, Criscione JC, et al. Alterations in transmural strains adjacent to ischemic myocardium during acute midcircumflex occlusion. *J Thorac Cardiovasc Surg.* 2005; 129(4):791–803. [PubMed: 15821645]
14. Shimkunas R, Makwana O, Spaulding K, Bazargan M, Khazalpour M, Takaba K, et al. Myofilament dysfunction contributes to impaired myocardial contraction in the infarct border zone. *Am J Physiol Heart Circ Physiol.* 2014; 307(8):H1150–8. [PubMed: 25128171]
15. Zhang P, Guccione J, Nicholas S, Walker J, Crawford P, Shamal A, et al. Endoventricular patch plasty for dyskinetic anteroapical left ventricular aneurysm increases systolic circumferential shortening in sheep. *The Journal of Thoracic and Cardiovascular Surgery.* 2007; 134(4):1017–1024. [PubMed: 17903523]
16. Llaneras MR, Nance ML, Streicher JT, Lima JA, Savino JS, Bogen DK, et al. Large animal model of ischemic mitral regurgitation. *Ann Thorac Surg.* 1994; 57(2):432–9. [PubMed: 8311608]
17. Kelley ST, Malekan R, Gorman JH 3rd, Jackson BM, Gorman RC, Suzuki Y, et al. Restraining infarct expansion preserves left ventricular geometry and function after acute anteroapical infarction. *Circulation.* 1999; 99(1):135–42. [PubMed: 9884390]
18. Wrazidlo W, Brambs HJ, Lederer W, Schneider S, Geiger B, Fischer C. An alternative method of three-dimensional reconstruction from two-dimensional CT and MR data sets. *Eur J Radiol.* 1991; 12(1):11–6. [PubMed: 1999203]
19. Dubois, E. The estimation of the surface area of the body.. In: Dubois, E., editor. *Basal metabolism in health and disease.* Lea and Febiger; Philadelphia, PA: 1936. p. 125-144.
20. Zoghbi W. Recommendations for evaluation of the severity of native valvular regurgitation with two-dimensional and doppler echocardiography. *Journal of the American Society of Echocardiography.* 2003; 16(7):777–802. [PubMed: 12835667]
21. Sacco JJ, Botten J, Macbeth F, Bagust A, Clark P. The average body surface area of adult cancer patients in the UK: a multicentre retrospective study. *PLoS ONE.* 2010; 5(1):e8933. [PubMed: 20126669]
22. Guttman MA, Zerhouni EA, McVeigh ER. Analysis and visualization of cardiac function from MR images. *IEEE Comp Graph Appl.* 1997; 17:30–38.
23. Ozturk C, McVeigh ER. Four-dimensional B-spline based motion analysis of tagged MR images: introduction and in vivo validation. *Phys Med Biol.* 2000; 45(6):1683–702. [PubMed: 10870718]
24. Kleinbaum, DG. *Applied regression analysis and other multivariable methods.* 4 ed.. Thomson Brooks/Cole Publishing; Belmont: 2008.

25. Kramer CM, Lima JA, Reichek N, Ferrari VA, Llaneras MR, Palmon LC, et al. Regional differences in function within noninfarcted myocardium during left ventricular remodeling. *Circulation*. 1993; 88(3):1279–88. [PubMed: 8353890]
26. Pilla JJ, Koomalsingh KJ, McGarvey JR, Witschey WR, Dougherty L, Gorman JH 3rd, et al. Regional myocardial three-dimensional principal strains during postinfarction remodeling. *Ann Thorac Surg*. 2015; 99(3):770–8. [PubMed: 25620591]
27. Langer F, Rodriguez F, Cheng A, Ortiz S, Harrington KB, Zasio MK, et al. Alterations in lateral left ventricular wall transmural strains during acute circumflex and anterior descending coronary occlusion. *Ann Thorac Surg*. 2007; 84(1):51–60. [PubMed: 17588382]
28. Fung, YC.; Tong, P. Classical and computational solid mechanics. World Scientific Publishing Co. Pte. Ltd.; Singapore: 2001.
29. Zuern CS, Krumm P, Wurster T, Kramer U, Schrieck J, Henning A, et al. Reverse left ventricular remodeling after percutaneous mitral valve repair: strain analysis by speckle tracking echocardiography and cardiac magnetic resonance imaging. *Int J Cardiol*. 2013; 168(5):4983–5. [PubMed: 23911275]
30. Jackson BM, Gorman JH, Moainie SL, Guy TS, Narula N, Narula J, et al. Extension of borderzone myocardium in postinfarction dilated cardiomyopathy. *J Am Coll Cardiol*. 2002; 40(6):1160–7. discussion 1168–71. [PubMed: 12354444]
31. Guccione JM, Moonly SM, Moustakidis P, Costa KD, Moulton MJ, Ratcliffe MB, et al. Mechanism underlying mechanical dysfunction in the border zone of left ventricular aneurysm: a finite element model study. *Ann Thorac Surg*. 2001; 71(2):654–62. [PubMed: 11235723]
32. Dispersyn G, Mesotten L, Meuris B, Maes A, Mortelmans L, Flameng W, et al. Dissociation of cardiomyocyte apoptosis and dedifferentiation in infarct border zones. *European Heart Journal*. 2002; 23:849–857. [PubMed: 12042006]
33. Narula N, Narula J, Zhang P, Haider N, Raghunath P, Britten R, et al. Is the myofibrillarlytic myocyte a forme fruste apoptotic myocyte? *Ann Thorac Surg*. 2005; 79:1333–1337. [PubMed: 15797072]
34. Wilson EM, Moainie SL, Baskin JM, Lowry AS, Deschamps AM, Mukherjee R, et al. Region- and type-specific induction of matrix metalloproteinases in post-myocardial infarction remodeling. *Circulation*. 2003; 107(22):2857–63. [PubMed: 12771000]
35. Mukherjee R, Mingoia JT, Bruce JA, Austin JS, Stroud RE, Escobar GP, et al. Selective spatiotemporal induction of matrix metalloproteinase-2 and matrix metalloproteinase-9 transcription after myocardial infarction. *Am J Physiol Heart Circ Physiol*. 2006; 291(5):H2216–28. [PubMed: 16766634]
36. Sawicki G, Leon H, Sawicka J, Sariahmetoglu M, Schulze CJ, Scott PG, et al. Degradation of myosin light chain in isolated rat hearts subjected to ischemia reperfusion injury: a new intracellular target for matrix metalloproteinase-2. *Circulation*. 2005; 112(4):544–52. [PubMed: 16027249]
37. Gao CQ, Sawicki G, Suarez-Pinzon WL, Csont T, Wozniak M, Ferdinandy P, et al. Matrix metalloproteinase-2 mediates cytokine-induced myocardial contractile dysfunction. *Cardiovasc Res*. 2003; 57(2):426–33. [PubMed: 12566115]
38. Ifkovits JL, Tous E, Minakawa M, Morita M, Robb JD, Koomalsingh KJ, et al. Injectable hydrogel properties influence infarct expansion and extent of postinfarction left ventricular remodeling in an ovine model. *Proc Natl Acad Sci U S A*. 2010; 107(25):11507–12. [PubMed: 20534527]
39. Hess AT, Zhong X, Spottiswoode BS, Epstein FH, Meintjes EM. Myocardial 3D strain calculation by combining cine displacement encoding with stimulated echoes (DENSE) and cine strain encoding (SENC) imaging. *Magn Reson Med*. 2009; 62(1):77–84. [PubMed: 19322795]
40. Pimentel DR, Adachi T, Ido Y, Heibeck T, Jiang B, Lee Y, et al. Strain-stimulated hypertrophy in cardiac myocytes is mediated by reactive oxygen species-dependent Ras S-glutathiolation. *J Mol Cell Cardiol*. 2006; 41(4):613–22. [PubMed: 16806262]

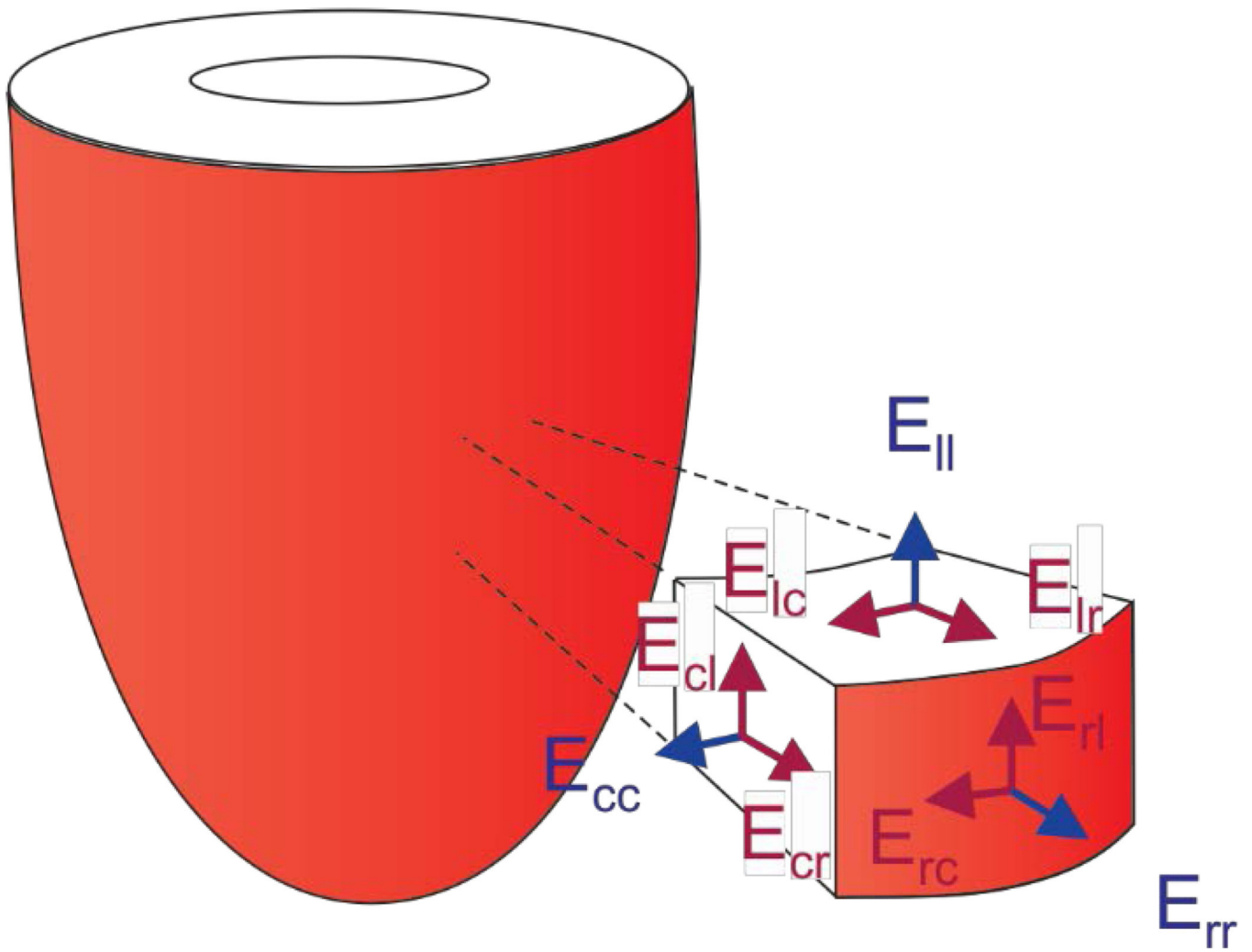
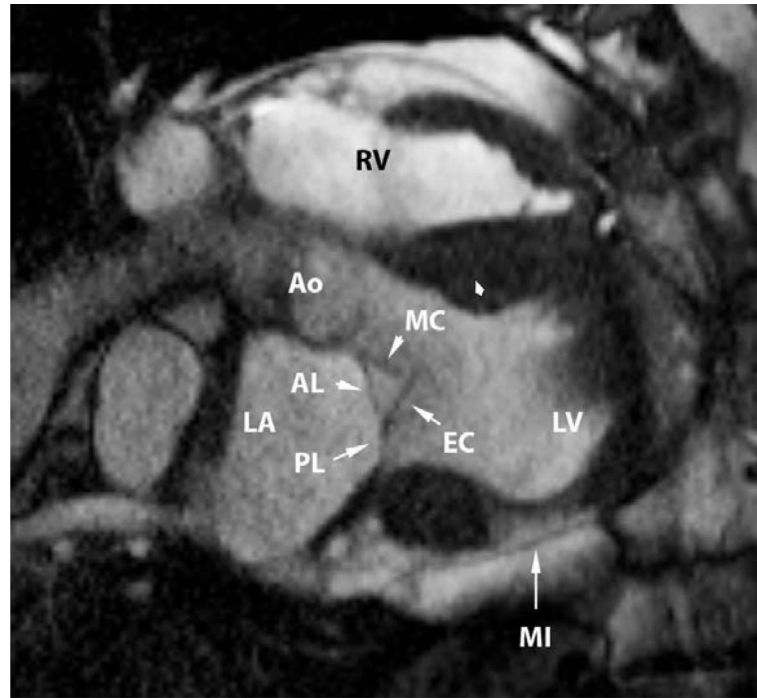
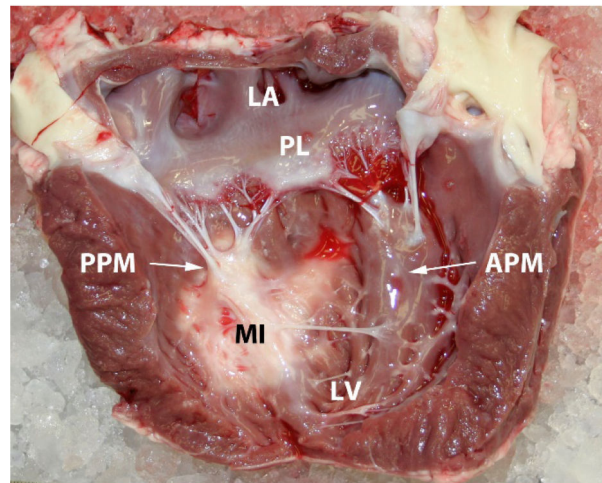


Figure 1. Diagram showing normal (blue) and shear (dark red) strain components in an exploded portion of the LV wall.



A.



B.

Figure 2.
Cine MRI (A) and post-mortem photograph (B) of typical postero-lateral MI.

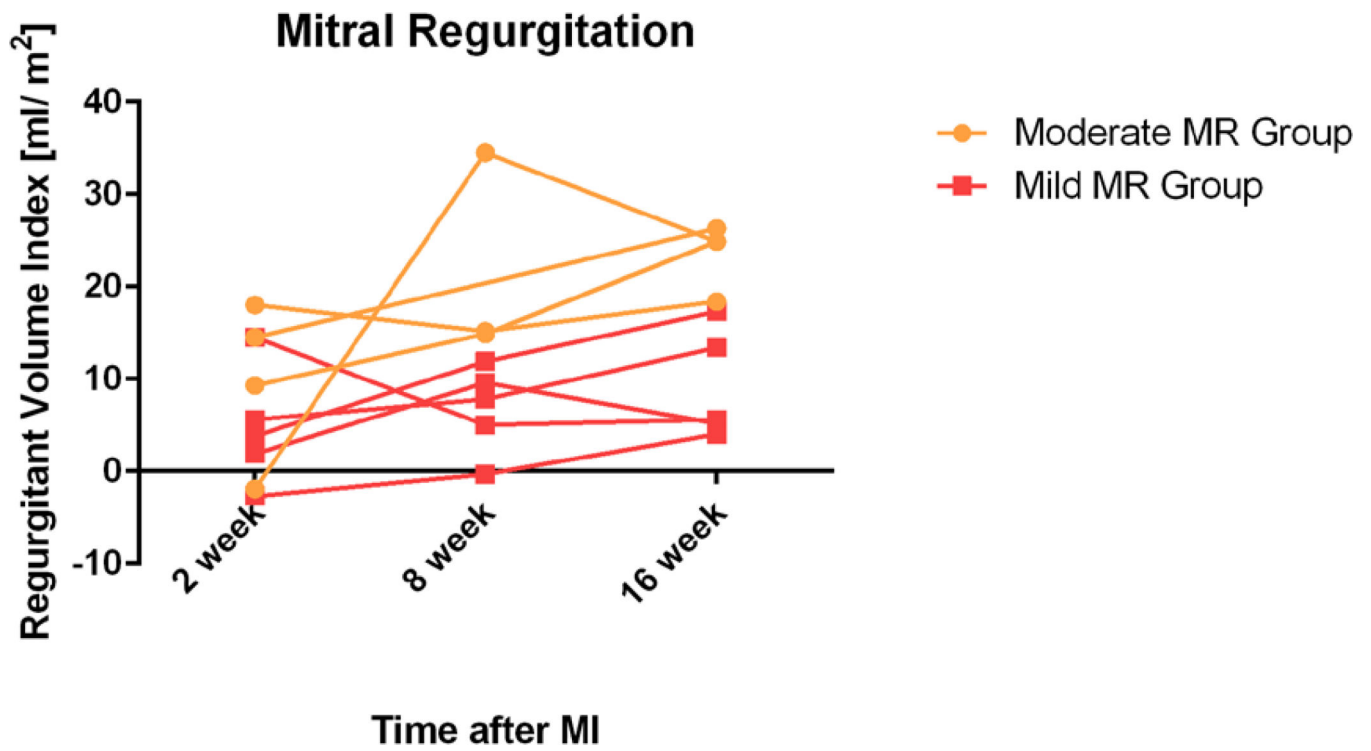


Figure 3. The change in RegurgVolume Index over time. Separate plots are shown for groups with mild and moderate ischemic mitral regurgitation (see text). Note that this data was previously presented. [6]

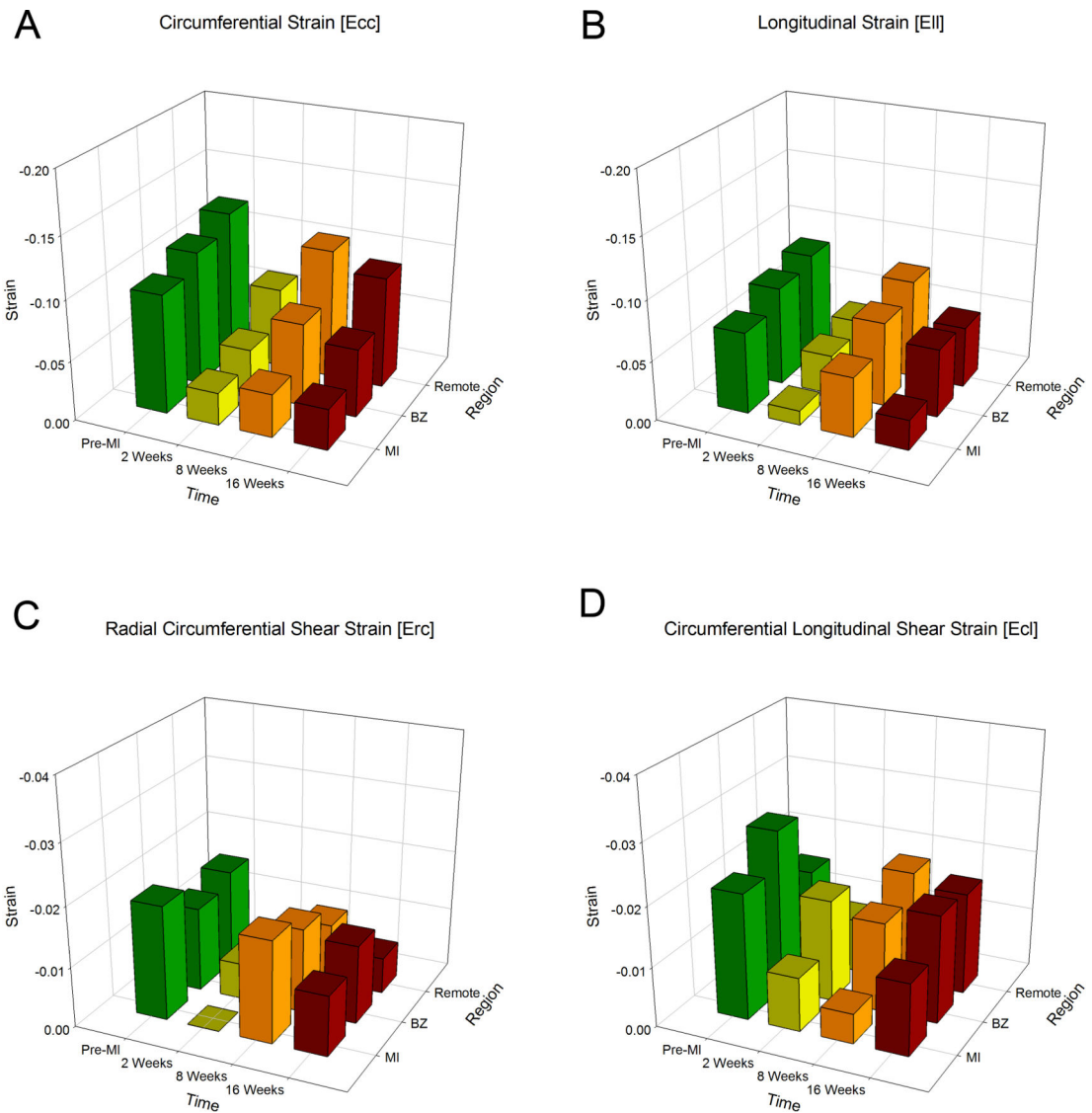


Figure 4. 3 dimensional plots of regional normal and shear strains after postero-lateral MI. Circumferential (A), longitudinal (B), radial-circumferential shear (C) and circumferential-longitudinal shear (D) strains are shown. In each case, time is on the X axis, region is on the Z axis and strain is on the Y (vertical) axis.

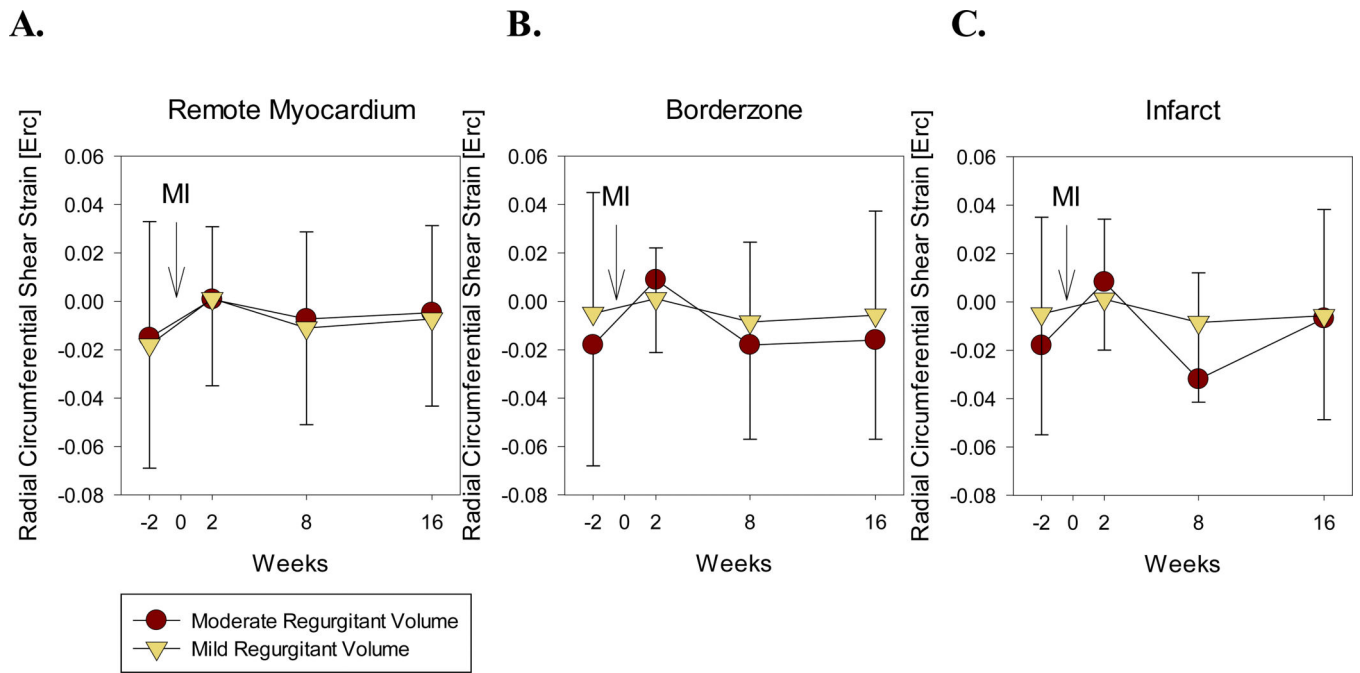


Figure 5. Effect of CIMR on radial circumflex shear strain (Erc) after posterolateral MI in the remote myocardium (A), borderzone (B) and infarct (C). Separate plots are shown for groups with mild and moderate ischemic mitral regurgitation (see text) although RegurgVolume Index was used as a continuous variable to calculate the statistical effect of CIMR.

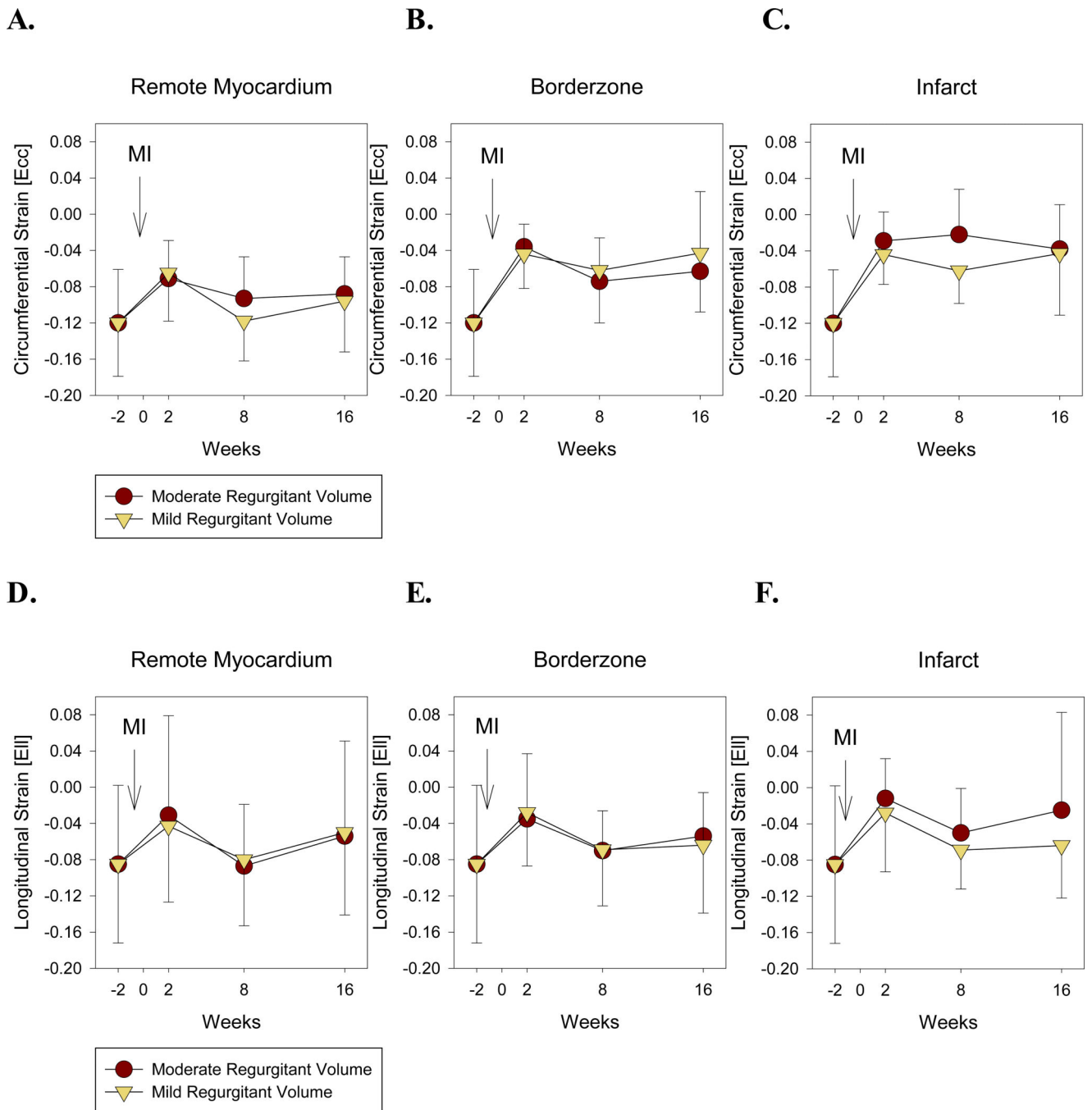


Figure 6. Effect of CIMR on circumflex (Ecc) and longitudinal (EII) strain after posterolateral MI. Ecc is seen in the remote myocardium (A), borderzone (B) and infarct (C) and EII is seen in the remote myocardium (D), borderzone (E) and infarct (F). The format is similar to **Figure 5**.

Table 1

Sheep weight, LV pressure, and LV volume 2 weeks before and 2, 8 and 16 weeks after postero-lateral MI.

	Pre-MI	2 Weeks post-MI	8 Weeks post-MI	16 Weeks post-MI
Animal weight [Kg]	53.2±4.4	53.9±27	59.4±2.4 ^{*†}	67.0±4.5 ^{*‡}
LV Pressure at ED [mm Hg]	5.7±1.3	6.9±1.5	6.5±1.4	6.6±2.6
LV Pressure at ES [mm Hg]	90.8±3.0	88.4±10.8	93.4±4.1	88.0±5.6
LV Volume at ED [ml]	83.9±17.1	109.8±15.7 [*]	122.5±22.4 [*]	132.3±22.7 ^{*†}
LV Volume at ES [ml]	40.4±10.3	61.2±15.5 [*]	63.6±16.1 [*]	69.4±2.6 [*]

Note that this data was previously presented. [6]

* p<0.05 vs Week 0

† p<0.05 vs Week 2 and

‡ p<0.05 vs Week 8.

Table 2

Strain in the circumflex (E_{cc}) and longitudinal (E_{ll}) directions by remote, borderzone (BZ) and infarct (MI) region 2 weeks before and 2, 8 and 16 weeks after postero-lateral MI.

		Pre-MI	2 Weeks post MI	8 Weeks post MI	16 Weeks post MI
E_{cc}	Remote	-0.125+0.059	-0.067+0.050 *	-0.108+0.047 * [†]	-0.093+0.052 * [†] [‡]
	BZ	-0.112+0.056	-0.038+0.042 *	-0.069+0.042 * [†]	-0.057+0.054 * [†]
	MI	-0.099+0.052	-0.027+0.032 *	-0.036+0.052 *	-0.034+0.050 *
E_{ll}	Remote	-0.089+0.088	-0.039+0.094 *	0.082+0.071 [†]	-0.051+0.096 * [†] [‡]
	BZ	-0.082+0.090	-0.033+0.056 *	-0.070+0.054 [†]	-0.057+0.078 * [†]
	MI	-0.068+0.069	-0.012+0.044 *	-0.050+0.049 [†]	-0.025+0.054 *

* p<0.05 vs Week 0

[†] p<0.05 vs Week 2 and

[‡] p<0.05 vs Week 8.

Table 3

Shear strains (E_{rc} , E_{rl} , and E_{lc}) by remote, borderzone (BZ) and infarct (MI) region 2 weeks before and 2, 8 and 16 weeks after postero-lateral MI.

		Pre-MI	2 Weeks post MI	8 Weeks post MI	16 Weeks post MI
E_{rc}	Remote	-0.016+0.049	-0.001+0.034 [*]	-0.010+0.039 ^{*†}	-0.006+0.036 [*]
	BZ	-0.014+0.050	-0.006+0.028 [*]	-0.014+0.037 [‡]	-0.013+0.042 [‡]
	MI	-0.019+0.046	-0.000+0.026 [*]	-0.017+0.044 [‡]	-0.010+0.041
E_{rl}	Remote	-0.002+0.069	-0.001+0.047	-0.008+0.066 [*]	-0.004+0.052 ^{*†}
	BZ	-0.020+0.072	-0.009+0.043	-0.021+0.059	-0.014+0.061
	MI	-0.017+0.053	-0.004+0.043	-0.013+0.045	-0.025+0.061 [‡]
E_{lc}	Remote	-0.016+0.061	-0.009+0.035 [*]	-0.019+0.041 [‡]	-0.017+0.045 [‡]
	BZ	-0.027+0.057	-0.017+0.029	-0.015+0.047 [*]	-0.018+0.045
	MI	-0.021+0.038	-0.009+0.031 [*]	-0.005+0.039 [*]	-0.012+0.053

‡-p<0.05 vs Week 8.

* p<0.05 vs Week 0

† p<0.05 vs Week 2 and